Supplementary Figure 1. ESI/MS/MS analyses of native and de-acetylated S2A. *Panel A*, Positive ESI mass spectra of native (N) and de-acetylated (DA) non-active S2A were obtained, and demonstrated a shift of approximately two acetyl groups (84 amu) when comparing major intact GPL ions (i.e. *m/z* 1595 vs. *m/z* 1511, and *m/z* 1561 vs. *m/z* 1477). *Panel B*, Major intact GPL ions were selected for collisionally activated dissociation (CAD). At a collision energy of 20 eV, product ions were produced, signifying the GPL ion with a loss of sugar moieties.

Supplementary Figure 2. Partial 1D ^{1}H NMR spectrum of S2A. Four dominant –OCH_3 signals and two dominant signals from the acetyl CH_3 groups could be observed for native S2A.

Supplementary Figure 3. Positive ESI mass spectra analyses of native and de-acetylated NS3. When comparing the *m/z* values for native (N) and de-acetylated (DA) intact GPL ions, a shift of approximately one acetyl group (42 amu) was observed (*m/z* 1233 vs. *m/z* 1191, and *m/z* 1246 vs. *m/z* 1205). There was another ion (*m/z* 1219) that was observed in both the N and DA spectra indicating the non-acetylated nsGPL that also comprises NS3. All relevant ions are circled.

Supplementary Figure 4. 1D ^{1}H NMR spectrum of NS2 in $CDCl_3$. *Panel A*, Full spectrum. *Panels B-F*, Expansions of select regions in (A) showing signal assignments for the 6-deoxytalose (dT) and rhamnose (R) residues.

Supplementary Figure 5. 2D ^{1}H-^{1}H NMR spectrum of NS2 in $CDCl_3$. Panel A, The H1-H2 cross-peaks for the 6-deoxytalose (dT) and the rhamnose (R) were used to initiate signal assignments in each residue (traces shown). Panel B, 2D ^{1}H-^{1}H ROESY spectrum of NS2 showing ROEs for $H1_R$, $H1_{dT}$, and $H4_{dT}$. SC denotes correlations to side-chain nuclei. R: rhamnose; dT: 6-deoxytalose.

Assignment of ^{1}H chemical shifts, anomeric configuration and substitution pattern for native NS2. The 1D ^{1}H NMR spectrum of NS2 contains two anomeric proton signals at 5.051 ppm and 4.798 ppm (Supplementary Table 1; Supplementary Fig. 5A, 5B). These signals gave identical integrations, and both were split by a small $^3J_{H1,H2}$ coupling (1.7 Hz and 1.8 Hz, respectively). Analysis of the 2D ^{1}H-^{1}H COSY spectrum (Supplementary Fig. 6A) provided chemical shift assignments of all non-anomeric protons in each residue (Supplementary Fig. 5B-F), and more detailed interpretation of these signals in the 1D spectrum yielded a complete set of $^3J_{HH}$ values in each residue (Supplementary Table 2). Absolute configurations of the residues were not confirmed; it is assumed they were in the L-configuration. Anomeric configurations were confirmed by comparing $^3J_{H1,H2}$ values in the NS2 6-deoxytalose and rhamnose with those observed in standard talo- and mannopyranosyl rings and were in agreement with the α-anomers.

The 1D ^{1}H NMR spectrum of NS2 contained four intense singlets (Supplementary Fig. 5A, 5C) that gave identical integrations (three protons each), consistent with CH_3 groups. Three of these signals were observed at 3.4-3.5 ppm and were assigned to methyl ether (-OCH_3) protons (Supplementary Table 1). The remaining singlet at 2.177 was assigned to the CH_3 of an acetyl group. Analysis of the $H2_{dT}$ and $H2_R$ multiplets revealed the presence of $^3J_{HCOH}$ couplings in both cases (7.9 Hz, and 2.3 Hz, respectively; $CDCl_3$ solvent), showing that OH2 in both residues is unsubstituted (Supplementary Table 2). Since both residues are 6-deoxyhexopyranosyl rings, the remaining four OH groups (OH3 and OH4 of both residues) must therefore be substituted, since four CH_3 signals were observed.

To determine the substitution pattern, two approaches were taken. ^{1}H chemical shift differences were calculated for the NS2 6-deoxytalose and rhamnose residues, and for standard unsubstituted talo- and mannopyranosyl residues, using H1 as the reference signal. Since OH2 in both residues is unsubstituted, δ_{H1}-δ_{H2} serves as a reasonable internal control, which is confirmed by the good agreement

observed between the NS2 6-deoxytalose and the α-talo standard, and between the NS2 rhamnose and the α-manno standard (Supplementary Table 3) (these differences also confirm the anomeric configuration of the NS2 6-deoxytalose and rhamnose). Values of δ_{H1}-δ_{H3} and δ_{H1}-δ_{H4} in the NS2 6-deoxytalose and rhamnose are *more positive* in three cases than the *positive* difference calculated in the reference compound, whereas in one case (δ_{H1}-δ_{H4} of the NS2 6-deoxytalose), the difference is *negative* compared to a *positive* difference calculated in the reference. These results support the conclusion that OH3 and OH4 of NS2 rhamnose, and OH3 of NS2 6-deoxytalose are substituted as methyl ethers, and the remaining site, OH4 of 6-deoxytalose, is acetylated. *O*-Methylation of a CH-OH fragment thus induces a modest upfield shift of the CH proton, whereas *O*-acetylation induces a significant downfield shift.

The above substitution pattern was supported by an analysis of the ^{1}H-^{1}H 2D ROESY spectrum of NS2 (Supplementary Fig. 6B). Inspection of the $H4_{dT}$ cross-peaks revealed strong correlations to H3 and H5, a moderate correlation to the most upfield ether $-OCH_3$ (presumably at O3), and a very weak correlation to the acetyl CH_3. This pattern is consistent with the proposed substitutions in the NS2 6-deoxytalose. In this interpretation, it is assumed that the acetyl CH_3 is, on average, relatively far removed from H4 due to conformation about the C4-O4 bond, and that conformation about the C3-O3 bond results in an average orientation of the CH_3 that places it relatively close to H4. The ROESY data also confirm free –OH groups in the NS2 6-deoxytalose and rhamnose, since H1 in both residues exhibits an NOE to the corresponding OH2 proton.

Supplementary Table 1

Table 1. ^{1}H chemical shifts of sample NS2

residue	chemical shift (ppm)									
	H1	H2	H3	H4	H5	H6	OH2	CH_3 (1) (ether)	CH_3 (2) (ether)	CH_3 (acetyl)
deoxyTalo (dT)	5.051	3.802	3.562	~5.307	3.950	1.158	2.790	3.418		2.177
Rhamno (R)	4.798	4.002	3.452	3.057	3.619	~1.26	2.633	3.525	3.468	

[a]In $CDCl_3$; 22 °C; chemical shifts referenced to the internal residual $CHCl_3$ signal (7.270 ppm).

Supplementary Table 2

Table 2. ^{1}H-^{1}H spin-couplings in sample NS2

residue	^{1}H-^{1}H spin coupling (Hz)[a]						
	$^{3}J_{H1,H2}$	$^{3}J_{H2,H3}$	$^{3}J_{H3,H4}$	$^{3}J_{H4,H5}$	$^{3}J_{H5,H6}$	$^{4}J_{H2,H4}$	$^{3}J_{H2,OH2}$
deoxyTalo (dT)	1.7	~3.1	~3.1	~1.2	5.7	1.2	7.9
Rhamno (R)	1.8	3.4	9.1	~9.5	5.8		2.3
α-Talo[b]	1.9	3.2	3.2	1.3		1.4	
β-Talo[b]	1.2	3.2	3.3	1.2		1.2	
α-Talo[c]	~1.9	3.4	~3.5	~1.3			
α-Manno[c]	1.8	3.5	9.5				
β-Manno[c]	0.9	3.2	9.6				

[a]In Hz ± 0.1 unless otherwise noted; in $CDCl_3$; 22° C. [b]Data for α- and β-D-talopyranoses taken from Ref. 1. [c]Data for methyl α-D-talopyranosides and methyl α- and β-D-mannopyranosides, taken from Ref. 2.

Ref. 1: Snyder, J. R., Johnston, E. R., and Serianni, A. S. (1989) *J Am Chem Soc* **111**, 2681-2687

Ref. 2: Podlasek, C. A., Wu, J., Stripe, W. A., Bondo, P. B., and Serianni, A. S. (1995) *J Am Chem Soc* **117**, 8635-8644

Supplementary Table 3

Table 3. ^{1}H chemical shift differences for residues 6-deoxytalose (dT) and rhamnose (R) in NS2, and for unsubstituted manno- and talopyranosyl rings.

residue	^{1}H chemical shift difference (ppm)		
	δH1-δH2	δH1-δH3	δH1-δH4
dT	1.25	1.49	-0.26
α-Talo[a]	1.41	1.32	~1.34
β-Talo[a]	0.87	1.00	~0.95
R	0.80	1.35	1.74
α-Manno[b]	0.83	1.00	1.12
β-Manno[b]	0.59	0.94	1.01

[a]Data for α- and β-D-talopyranoses taken from Ref. 1. [b]Data for methyl α- and β-D-mannopyranosides taken from Ref. 2

Ref. 1: Snyder, J. R., Johnston, E. R., and Serianni, A. S. (1989) *J Am Chem Soc* **111**, 2681-2687

Ref. 2: Podlasek, C. A., Wu, J., Stripe, W. A., Bondo, P. B., and Serianni, A. S. (1995) *J Am Chem Soc* **117**, 8635-8644

Supplementary Figure 1

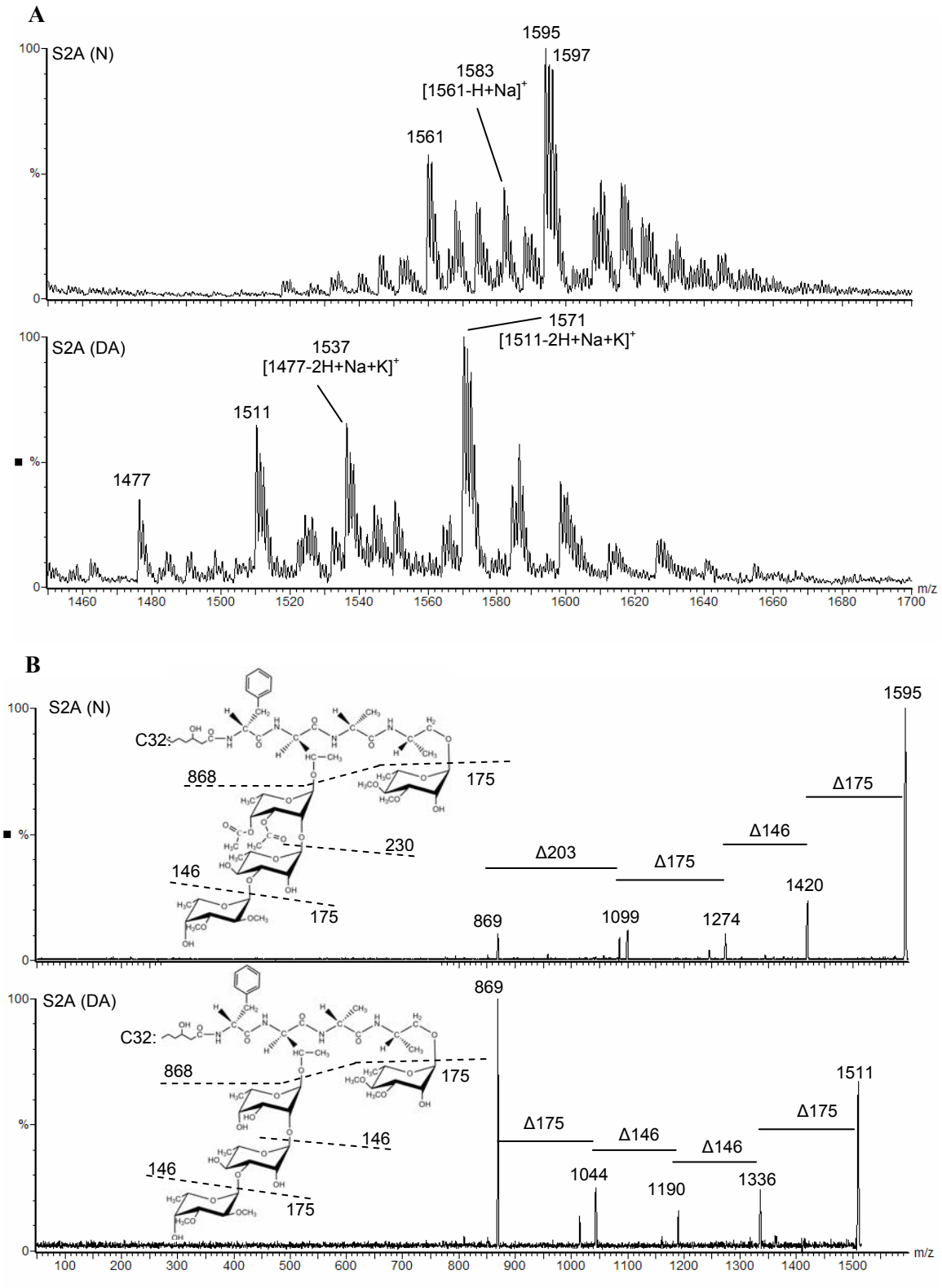

Supplementary Figure 2

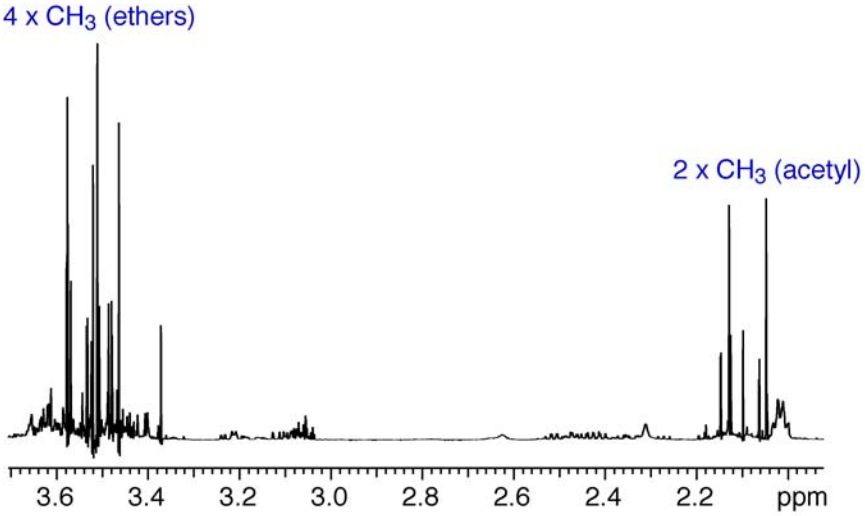

Supplementary Figure 3

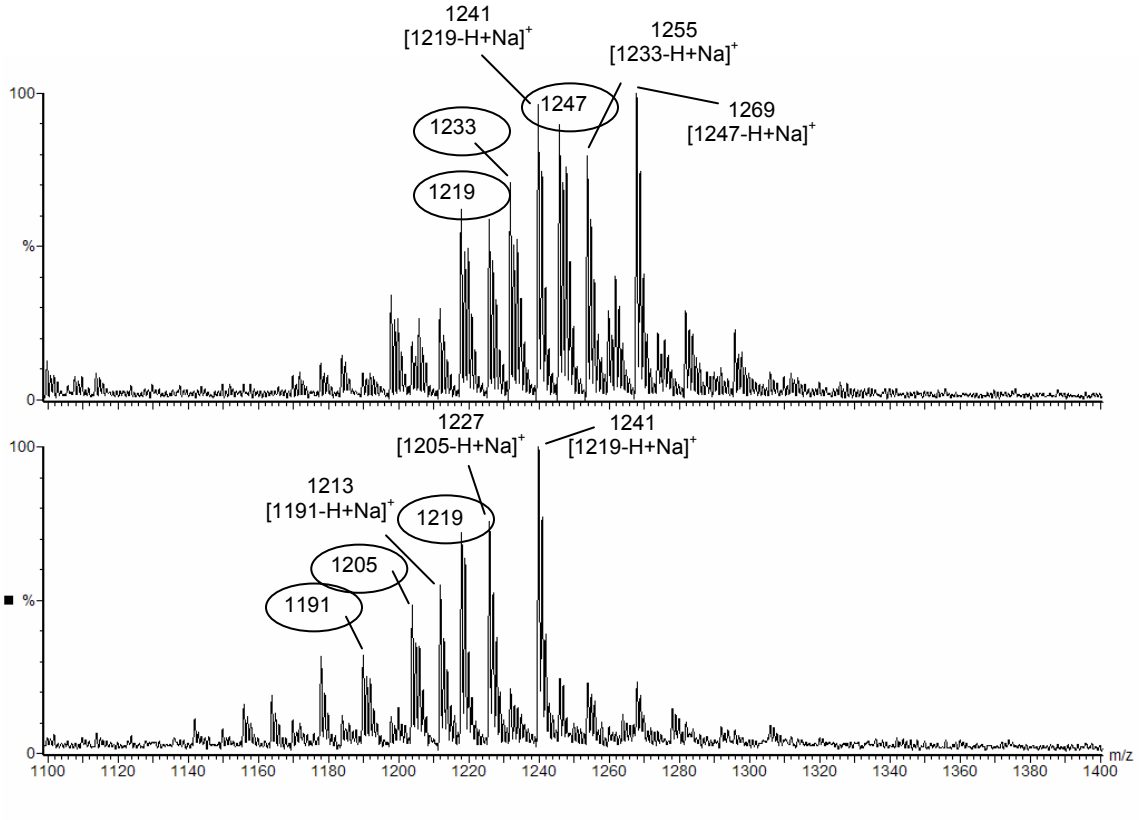

Supplementary Figure 4

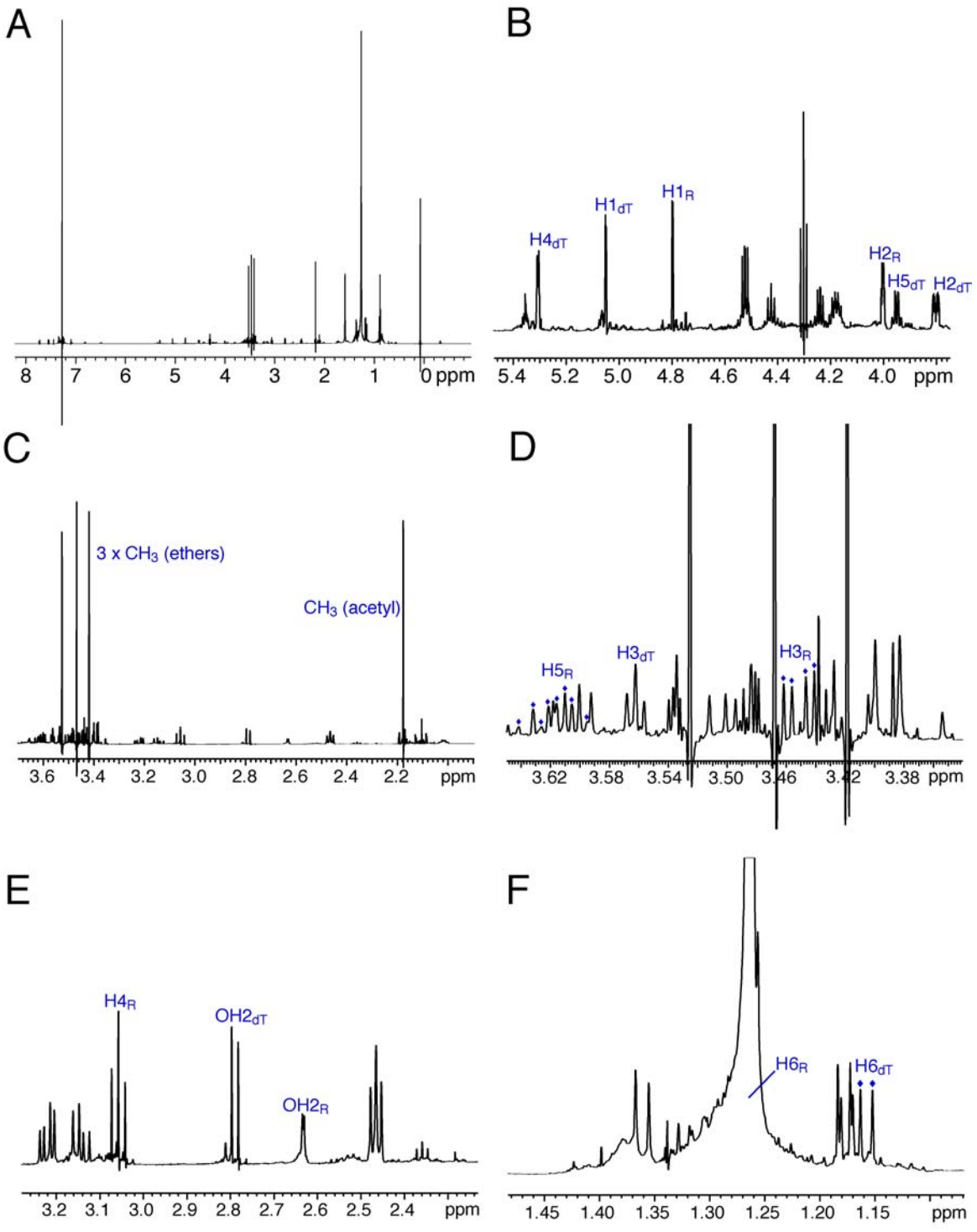

Supplementary Figure 5